# Kinetic Mechanism of Deoxyadenosine Kinase from *Mycoplasma* Determined by Surface Plasmon Resonance Technology†

Ewa Pol*,‡ and Liya Wang§

*Biacore AB, SE-754 50 Uppsala, Sweden, and Department of Molecular Biosciences, Section of Veterinary Medical Biochemistry, Swedish University of Agricultural Sciences, The Biomedical Centre, SE-751 23 Uppsala, Sweden*

*Received August 4, 2005; Revised Manuscript Received October 24, 2005*

ABSTRACT: Surface plasmon resonance (SPR) detection technology was employed to investigate the kinetic mechanism of deoxyadenosine kinase from *Mycoplasma mycoides* ssp. *mycoides* SC. In our experimental approach, the enzyme was attached to the sensor surface, the reactants were injected in the mobile phase, and the product−enzyme complex formation was measured using the fact that the rate of product formation exceeds that of its dissociation. The pre-steady-state analysis of deoxyguanosine phosphorylation showed the presence of a burst phase, which is consistent with product dissociation being a rate-limiting step. High activity of the immobilized enzyme was demonstrated by analyzing the reaction mixture eluted from the chip and by determining the Michaelis−Menten constants for several phosphate acceptors (e.g., deoxyadenosine) and phosphate donors (e.g., ATP) using SPR detection. These values were in good agreement with those reported previously [Wang, L. et al. (2001) *Mol. Microbiol. 42*, 1065−1073]. The bisubstrate initial rate pattern obtained was characteristic of a sequential kinetic mechanism. Because in the method applied here it is the mass change on the surface that is monitored, a new mathematical approach to interpreting product inhibition experiments was proposed. According to that approach, product inhibition studies, supported by product binding experiments, indicated that the reaction mechanism was of Bi Bi sequential ordered type, involving the formation of a ternary complex, in which ATP and deoxyadenosine bound sequentially, followed by a transfer of the phosphate group, and an ordered release of products with ADP dissociating before dAMP.

Deoxynucleoside kinases catalyze the transfer of a gamma phosphoryl group from nucleoside triphosphate to the 5′-OH group of a deoxyribonucleoside, which is a rate-limiting step in the salvage pathway as well as the prerequisite step in activation of nucleoside analogues used in chemotherapy (*1*, *2*). Since only limited and conflicting data concerning the kinetic mechanism of the deoxynucleoside kinase family are available, a clear understanding of the modes of substrate binding and enzymatic regulation in this family is highly desirable.

In this work, we go some distance toward explaining the kinetic mechanism of deoxyadenosine kinase (dAK)[1] from *Mycoplasma mycoides* ssp. *mycoides* small colony type (*3*), for which natural deoxynucleosides, deoxyadenosine (dAdo), deoxyguanosine (dGuo), and deoxycytidine (dCyd) are substrates, and nucleoside triphosphates, ATP, CTP, TTP, and UTP are phosphate donors. Our experimental approach to explaining the kinetic mechanism is based on surface plasmon resonance (SPR) detection (*4*, *5*). SPR response depends on a change in the refractive index in the close vicinity of the sensor surface and is proportional to the mass of the molecules bound on the surface (*6*). The experimental procedure involves immobilization of the enzyme onto the chip and a continuous delivery of the substrates, at a constant flow rate, to the enzyme. Therefore, the total concentration of the enzyme, as well as that of the substrates in the bulk, can be regarded as constant. It can also be assumed that, for the initial phase of the reaction, the concentration of the free substrate is almost identical to the concentration that is injected in the mobile phase and vastly exceeds that of the enzyme. Furthermore, if a mass change can be detected on the enzyme in the course of the reaction, then an enzymatic activity can be monitored using SPR technology. Such conditions occur, for instance, when the product is produced in a much faster way than it is released from the enzyme. In such a case, the increasing SPR response corresponds to the product formation on the enzyme. The rate of the reaction can thus be measured, since it is proportional to the rate of the enzyme−product complex formation.

† This work was supported by grants from the Swedish Medical Research Council and the Swedish Research Council for Environment, Agricultural Sciences and Spatial Planning.

* Corresponding author. Tel.: +46 18 675 889. Fax: +46 18 15 01 13. E-mail: ewa.pol@biacore.com.

‡ Biacore AB.

§ Swedish University of Agricultural Sciences.

[1] Abbreviations: app, subscript denoting an apparent rate constant; dAK, deoxyadenosine kinase; $k_1$, the association rate constant; $k_{-1}$, the dissociation rate constant; $k_2$, the rate constant for the conversion of the enzyme−substrate to the enzyme−product complex; $k_3$, the dissociation rate constant of the enzyme−product complex; $k_b$, the observed burst rate; $k_{ss}$, the observed steady-state rate; $k_{cat}$, turnover number; $K_I$, dissociation equilibrium constant; $K_m$, Michaelis−Menten constant; $K'_m$, here: Michaelis−Menten constant characterizing the multistep interaction in which the rate-limiting product dissociation step is omitted; RU, resonance unit; SPR, surface plasmon resonance; $V_{max}$, maximal rate of the catalytic reaction; $V'_m$, maximal rate of the multistep catalytic reaction in which the rate-limiting product dissociation step is omitted.

10.1021/bi0515523 CCC: $33.50 
Published on Web 12/17/2005

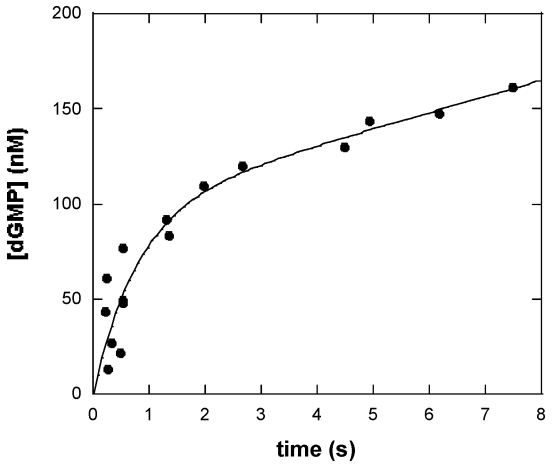


FIGURE 1: Pre-steady-state kinetics of phosphorylation of dGuo by dAK using ATP as a phosphate donor. A preincubated solution of dAK (5 $\mu$M) and $H^3$-dGuo (20 $\mu$M) was mixed with ATP (10 mM) and the reaction was stopped at various time points by adding 1 M HCl. A fitting to a biphasic equation gave the rate constants for exponential and linear phase of $1.3 \pm 0.5$ $s^{-1}$ and $0.09 \pm 0.07$ $s^{-1}$, respectively.

Table 1: Comparison of the $K'_m$ Values Determined by SPR Detection and by Radiometry

| variable substrate | fixed substrate | $K'_m$ (M) determined in Biacore | $K'_m$ (M) determined by radiometry (*6*) |
|---|---|---|---|
| ATP | dAdo | $(16 \pm 3) \times 10^{-6}$ | $(11 \pm 2) \times 10^{-6}$ |
| CTP | dAdo | $(21 \pm 4) \times 10^{-6}$ | $(22 \pm 4) \times 10^{-6}$ |
| TTP | dAdo | $(77 \pm 12) \times 10^{-6}$ | $(67 \pm 7) \times 10^{-6}$ |
| UTP | dAdo | $(135 \pm 26) \times 10^{-6}$ | $(176 \pm 12) \times 10^{-6}$ |
| dAdo | ATP | $(10 \pm 2) \times 10^{-6}$ | $(12 \pm 3) \times 10^{-6}$ |
| dGuo | ATP | $(20 \pm 4) \times 10^{-6}$ | $(21 \pm 4) \times 10^{-6}$ |
| dCyd | ATP | $(121 \pm 13) \times 10^{-6}$ | $(177 \pm 15) \times 10^{-6}$ |
| dAdo | CTP | $(18 \pm 3) \times 10^{-6}$ | N.D. |
| dGuo | CTP | $(19 \pm 2) \times 10^{-6}$ | N.D. |
| dCyd | CTP | $(146 \pm 18) \times 10^{-6}$ | N.D. |

[a] Measured values are given ± SE. The methods and buffers used in the determination of $K'_m$ are given in the Materials and Methods section. N.D., not determined.

A minimal kinetic scheme of dAK, derived in this work from a pre-steady-state experiment, showed that the product dissociation is a rate-limiting step of the reaction (Figure 1). Moreover, the Michaelis−Menten constants for several phosphate group donors and acceptors, determined from the initial slopes of the enzyme−product complex formation curves, were comparable to the constants determined previously (*3*) (Table 1), which, by indicating that the true rate of the product formation is measured on the chip, provides a firm ground for examining the kinetic mechanism of the enzyme-catalyzed reaction.

Information about the sequence of events on the enzyme was obtained by determining the initial velocity pattern and by performing the product inhibition experiments (*7*, *9*−*11*). However, in the product inhibition study, the initial slopes observed were no longer correlated with the initial rate of the product formation. Instead, the net mass change on the surface depended on two different events occurring simultaneously: the production of the product during the catalytic reaction and the binding of the product-inhibitor, added prior to the reaction, to the enzyme. To interpret adequately the results obtained from this type of experiment, a new approach to evaluating data is therefore called for, because, unlike the traditional methods measuring the overall rate of reaction, the method used in our experiments monitors the mass change on the enzyme. In this paper, we propose such a new approach in the form of a concrete mathematical framework. The equations describing the effects of the product inhibitors, offered in the next section, can be viewed as the first step toward a better understanding of the complex nature of the processes involved.

*Theoretical Background.* The enzymatic reaction studied involves two substrates and two products, but since one of the substrates is kept at a saturating level, the reaction scheme can be simplified by omitting the second substrate and product. By adopting the Briggs-Haldane steady-state approach (*12*, *13*), the reaction can be described as follows:

$$E + S \underset{k_{-1}}{\overset{k_1}{\rightleftharpoons}} ES \xrightarrow{k_2} EP \xrightarrow{k_3} E + P \qquad (1)$$

where E denotes the enzyme; $k_1$ and $k_{-1}$ denote the association and dissociation rate constants, respectively; $k_2$ denotes the rate constant for the conversion of the enzyme−substrate to the enzyme−product complex; and $k_3$ denotes the dissociation rate constant of the enzyme−product complex. It is assumed here that the reverse reaction converting product to substrate is negligible. For an isolated system, the rate, $v$, the Michaelis−Menten constant, $K_m$, the maximal rate, $V_{max}$, and the turnover number, $k_{cat}$, of the catalytic reaction presented by eq 1 can be calculated using the King-Altman and Cleland method (*7*−*10*):

$$v = \frac{k_2k_3/(k_2 + k_3)[E]_{tot}[S]}{(k_{-1} + k_2)/k_1k_3/(k_2 + k_3) + [S]}$$

$$K_m = (k_{-1} + k_2)/k_1k_3/(k_2 + k_3)$$

$$V_{max} = k_2k_3/(k_2 + k_3)[E]_{tot}$$

$$k_{cat} = k_2k_3/(k_2 + k_3)$$

where $[E]_{tot}$ is the total enzyme concentration and [S] is the concentration of the substrate.

If $k_2 \gg k_3$ (i.e., if the product formation is much faster than the product dissociation), then

$$d[EP]/dt = k_2[ES] - k_3[EP] \approx k_2[ES]$$

The last step in Scheme 1 can be omitted, thus reducing the reaction to a simple bimolecular binding with a subsequent conversion of the bound substrate into the product:

$$E + S \underset{k_{-1}}{\overset{k_1}{\rightleftharpoons}} ES \xrightarrow{k_2} EP \qquad (2)$$

The equations describing $v$, $K_m$, $V_{max}$, and $k_{cat}$ can then be reformulated giving the values valid for eq 2. The symbol ′ is added to these constants to distinguish them from those already described above:

$$v' = \frac{k_2[E]_{tot}[S]}{(k_{-1} + k_2)/k_1 + [S]}$$

$$K'_m = (k_{-1} + k_2)/k_1$$

$$V'_{max} = k_2[E]_{tot}$$

$$k'_{cat} = k_2 \quad (3)$$

By substituting $(k_{-1} + k_2)/k_1$ for $K_m'$, and $k_2[E]_{tot}$ for $V'_{max}$, in eq 3, we obtain the Henry−Michaelis−Menten equation:

$$v' = V'_{max}[S]/(K'_m + [S]) \quad (4)$$

To apply SPR technology as a tool for the study of enzymatic activity, the substrate-to-product conversion must be connected to a mass change on the sensor surface. In our experimental approach, the net mass increase on the immobilized enzyme is monitored by taking advantage of the product dissociation being the rate-limiting step of the reaction. The total concentration of the immobilized enzyme is a sum of the concentrations of free and bound enzyme. The total free enzyme gives a baseline response and the molecule bound to the immobilized enzyme gives rise to the SPR response, *R*, which is measured in resonance units (RU) (*4*, *5*). The theoretical maximal response observed, $R_{max}$, is reached when no free enzyme is present on the sensor surface, i.e., when the enzyme is saturated. The observed initial binding slope of the product formation curve, d*R*/d*t*, corresponds to the initial rate of reaction, $v'$. The Biacore response is correlated to the amount of a molecule bound and is an indirect measure of the enzyme concentration in molar terms. We can therefore assume that $[E]_{tot} = R_{max}$ and that the concentration of the free enzyme, [E], is equal to $R_{max} - R$. Equation 4, expressed in Biacore terms, is then as follows:

$$v' = dR/dt = k_2R_{ES} = k_2R_{max}[S]/(K'_m + [S]) \quad (5)$$

where $R_{ES}$ is the steady-state response of the enzyme−substrate complex at infinite time when $dR/dt = 0$.

Underlying our theoretical considerations is the assumption that the substrate concentration on the sensor surface is equal to that injected in the mobile phase (*14*).

*Interpretation of Product Inhibition Experiments.* Product inhibition study is typically used to help to determine the kinetic mechanism of enzyme-catalyzed reaction (*7*, *9*−*11*). In a traditional experiment, net velocity of the substrate to product conversion is measured in the absence and in the presence of the preexisting product. This velocity is always lower in the presence of the product for the same substrate concentration and the way in which it decreases determines the type of inhibition. By examining the inhibition of each product versus each substrate, a specific inhibition pattern emerges that helps in identifying the kinetic mechanism.

If the release of the product is a rate-limiting step of a multistep reaction, the product inhibition can be studied by monitoring the product formation on the immobilized enzyme using SPR detection. However, in the presence of the preexisting product (that acts as an inhibitor), the net mass increase is not proportional to the rate of the reaction. In such a case, the increasing response consists of two components: the first arising from the accumulation of the product formed during the catalytic reaction, and the second arising from the binding of the initially added product. Then, the initial slopes of the binding curves obtained in the absence and in the presence of the product-inhibitor will differ.

In the remainder of this section, we outline a new mathematical account that allows the interpretation of the data obtained from the product inhibition study, in which the net mass increase of the product, formed during the catalytic reaction as well as added prior to it, is measured. As in the case of the classical method, the product inhibition pattern obtained using our account, should in principle reveal any kinetic mechanism involved. Since there are three different possible types of inhibition (noncompetitive, uncompetitive, and competitive), we shall consider each of them separately.

*Noncompetitive Product-Inhibitor.* A noncompetitive product-inhibitor binds to the enzyme independently of the substrate and with the same strength regardless of whether it binds before, simultaneously, or after the substrate has bound.

The following two binding events take place:

$$1.\ E + S \rightleftarrows ES, \text{ with } K'_m = [S][E]/[ES] \quad (6)$$

$$2.\ E_p + I \rightleftarrows EI, \text{ with } K_I = [I][E_p]/[EI] \quad (7)$$

where $E_p$ will henceforth be used to denote the enzyme fraction available for the binding of the product-inhibitor. Since the two binding events occur independently, the response observed is a sum of individual responses:

$$R = R_{ES} + R_{EI} \quad (8)$$

By substituting $R_{max} - R$ for [E], and $R_{ES}$ for [ES], and by rearranging eq 6, we obtain the following expression for the steady-state response of the enzyme−substrate complex at infinite time:

$$R_{ES} = [S](R_{max} - R)/K'_m \quad (9)$$

Similarly, by substituting $([S]R_{max}/K'_m - R)$ for $[E_p]$, and $R_{EI}$ for [EI], and by rearranging eq 7, we obtain the expression for the steady-state response of the enzyme−inhibitor complex at infinite time:

$$R_{EI} = I([S]R_{max}/K'_m - R)/K_I \quad (10)$$

The initial rate of product formation in the presence of the inhibitor is

$$v' = dR/dt = k_{2,app}R \quad (11)$$

where $k_{2,app}$ can be described as an apparent rate constant of the product formation in the presence of the product added.

Putting eqs 9 and 10 into eq 8 we get:

$$R = ([S]R_{max} - R)/K'_m + I([S]R_{max}/K'_m - R)/K_I$$

which ultimately leads to the equation:

$$R = [S]R_{max}(1 + [I]/K_I)/([S] + K'_m(1 + [I]/K_I)) \quad (12)$$

Finally, from eqs 11 and 12 we obtain the equation that characterizes the noncompetitive product-inhibitor:

$$v' = k_{2,app}R_{max}[S](1 + [I]/K_I)/([S] + K'_m(1 + [I]/K_I))$$

According to this equation, the apparent maximal initial binding rate, $k_{2,app}R_{max}$, and the apparent $K'_m$ value are

higher in the presence of the noncompetitive product-inhibitor, and both increase with the same factor: $1 + [I]/K_I$ (compare with eq 5).

The double reciprocal equation is as follows:

$$\frac{1}{v'} = \frac{K'_m}{k_{2,app}R_{max}[S]}\frac{1}{} + \frac{1}{k_{2,app}R_{max}\left(1 + \frac{[I]}{K_I}\right)} \qquad (13)$$

Thus, the linear pattern showing the effect of the noncompetitive inhibitor, obtained when $1/v'$ is plotted against 1/[S], will give parallel lines with the intercepts decreasing with the increasing inhibitor concentrations.

*Uncompetitive Product-Inhibitor*. The binding of the uncompetitive inhibitor requires a previous or simultaneous binding of the substrate to the enzyme. The binding events occurring in the presence of the uncompetitive inhibitor can be described as follows:

$$1.\ E + S \rightleftarrows ES, \text{ with } K'_m = [S][E]/[ES]$$

$$2.\ [E_p] + I \rightleftarrows EI, \text{ with } K_I = [I][E_p]/[EI]$$

For the uncompetitive inhibitor $[E_p] = [ES]$.

The steady-state concentrations of both the enzyme−substrate and enzyme−inhibitor complexes, expressed in Biacore terms as responses, are

$$R_{ES} = [S](R_{max} - R)/K'_m \qquad (14)$$

and

$$R_{EI} = [I]R_{ES}/K_I = [I][S](R_{max} - R)/(K'_m K_I) \qquad (15)$$

In the case in which the product-inhibitor binds to the enzyme after the substrate, the total response observed is a sum of individual responses, since the binding of S and I is not mutually exclusive:

$$R = R_{ES} + R_{EI} = [S](R_{max} - R)/K'_m + [I][S](R_{max} - R)/(K'_m K_I)$$

This yields:

$$R = [S]R_{max}/([S] + K'_m/(1 + [I]/K_I))$$

Inserting this expression into eq 11 we finally obtain:

$$v' = k_{2,app}[S]R_{max}/([S] + K'_m/(1 + [I]/K_I))$$

In the case when the uncompetitive product-inhibitor binds to the enzyme after the substrate has bound, the apparent maximal initial binding rate remains unchanged and the apparent $K'_m$ value decreases with factor $1 + I/K_I$ (compare with eq 5).

The double reciprocal plot ($1/v'$ plotted against 1/[S]), described by the following equation, will give the lines with the common intercept and the slopes that decrease with the increasing inhibitor concentrations:

$$\frac{1}{v'} = \frac{K'_m}{k_{2,app}R_{max}\left(1 + \frac{[I]}{K_I}\right)} \times \frac{1}{[S]} + \frac{1}{k_{2,app}R_{max}}$$

Let us also consider a situation in which the uncompetitive inhibitor binds directly to the ES complex before any product is formed. The amount of the enzyme−substrate complex that can be converted into the enzyme−product complex is diminished by the amount of the enzyme−substrate−product complex. Translating all this to responses we get:

$$R^{\ddagger}_{ES} = R_{ES} - R_{EI} \qquad (16)$$

where $R^{\ddagger}_{ES}$ is the steady-state response of the enzyme−substrate complex that produces the product. Replacing $R_{ES}$ and $R_{EI}$ in eq 16 by eqs 14 and 15, respectively, and substituting $R^{\ddagger}_{ES}$ for $R$ in eq 11, we obtain:

$$v' = k_{2,app}\frac{[S]R_{max}(1 - [I]/K_I)/(1 + [I]/K_I)}{[S] + K'_m/(1 + [I]/K_I)}$$

The above equation describes the effect of the simultaneous binding of the uncompetitive inhibitor and the substrate to the enzyme. The apparent initial maximal binding rate increases or decreases depending on the [I] and $K_I$ values, and the apparent $K'_m$ value decreases with the factor $1 + [I]/K_I$ (compare with eq 5).

The double reciprocal plot ($1/v'$ plotted against 1/[S]) is described by the following equation:

$$\frac{1}{v'} = \frac{K'_m}{k_{2,app}R_{max}\left(1 - \frac{[I]}{K_I}\right)}\frac{1}{[S]} + \frac{\left(1 + \frac{[I]}{K_I}\right)}{k_{2,app}R_{max}\left(1 - \frac{[I]}{K_I}\right)} \qquad (17)$$

Both the slopes and the intercepts of this plot vary depending on the [I] and $K_I$ values.

*Competitive Product-Inhibitor*. The binding of the competitive inhibitor precludes the binding of the substrate. The competitive product-inhibitor competes for the same enzyme form and site as the substrate. The equation that describes this process is similar to that offered previously for two analytes competing for the same site on the immobilized ligand (*15*). By applying this equation to the case in which the product formed from the substrate during the catalytic reaction and the product added prior to it compete for the same binding site, we obtain the expression for the steady-state response in the presence of the competitive product inhibitor:

$$R = \frac{R_{max}([S] + [I]K'_m Mw2/(Mw1K_I))}{[S] + K'_m(1 + [I]/K_I)} \qquad (18)$$

where Mw1 and Mw2 are molecular weights of the product formed and added, respectively. The double-reciprocal equation obtained by inserting eq 18 into eq 11 and by taking the inverse expression is

$$\frac{1}{v'} = \frac{1 + K'_m(1 + [I]/K_I)/[S]}{k_{2,app}R_{max}(1 + [I]Mw2K'_m/([S]Mw1K_I))}$$

In the case in which $K_I \gg K'_m$, the differentiation of the curves obtained in the absence and in the presence of the preexisting product-inhibitor becomes difficult. Another difficulty lies in the higher degree of complexity of the

equation describing the process, which results in the nonlinear double reciprocal plot.

## MATERIALS AND METHODS

*Instrumentation.* Biacore S51 (Biacore AB, Uppsala, Sweden) was used for SPR studies aiming to determine the Michaelis−Menten constants and for the studies of the kinetic mechanism, whereas Biacore 3000 (Biacore AB) was used for analyzing the composition of reaction mixtures. Radioactivity was counted in a LS6500 multipurpose scintillation counter (Beckman Coulter AB, Stockholm, Sweden).

*Software.* Biacore S51 Control Software version 1.2 and Biacore 3000 Control Software version 4.0.1 were used for running the assays, whereas Biacore S51 Evaluation Software version 1.2, BIAevaluation version 4.1 and KaleidaGraph version 3.5 (Synergy Software, Reading, PA) were used for analyzing and fitting the data obtained.

*Enzyme, Substrates, and Products.* Deoxyadenosine kinase from *M. mycoides* ssp. *mycoides* SC was expressed in *Escherichia coli* as a fusion protein with an N-terminal 6X histidine tag and purified by metal affinity chromatography on a TALON resin (BD Biosciences Clontech, Mountain View, CA) as described previously (*3*). Active dAK is a homodimer, and the enzyme was used without the removal of the His-tag. Deoxynucleosides and deoxynucleotides were purchased from Sigma-Aldrich Sweden AB Stockholm, Sweden.

*Pre-Steady-State Kinetic Analysis.* Ten microliters of the mixture containing 5 $\mu$M enzyme and 20 $\mu$M tritium-labeled dGuo were placed into a well of the 96-well microtiter plate. Two micropipets provided with tips, one containing 5 $\mu$L of 10 mM ATP and the other containing 10 $\mu$L of 1 M HCl, were immersed in the enzyme/dGuo droplet. The reaction was started and stopped at multiple time points by a rapid addition of ATP and HCl, respectively. The time for each start and stop point was measured in milliseconds using a stopwatch on the site http://www.sikeston.k12.mo.us/gwilliams/stopwatch.html. To analyze the reaction products, 20 $\mu$L of the above mixture was first neutralized with 2 M NaOH and then spotted onto DE81 filter paper (Whatman plc, Brentford Middlesex, UK) and dried. The filters were washed three times with 0.005 M ammonium formate and once with water. The reactants were eluted with 0.5 mL of 0.1 M HCl and 0.2 M KCl, and after mixing the sample with scintillation fluid, the radioactivity was counted in a scintillation counter (Beckman AB). The data from the burst kinetic experiments were fit by nonlinear regression analysis to a biphasic equation:

$$[P] = [E](1 - \exp(-k_b t) + k_{ss} t)$$

where [P] is the concentration of product formed, [E] is the concentration of the active enzyme, $k_b$ is the observed burst rate, and $k_{ss}$ is the observed steady-state rate.

*Preparation of Sensor Surfaces.* Penta-His antibody (Qiagen Inc. Valencia, CA) was immobilized on the both spots of the flow cell (in Biacore S51) or on one flow cell (in Biacore 3000), using the standard amine coupling method (*16*). Coupling buffer was 0.01 M sodium acetate (pH 5.0), and running buffer was 0.01 M Hepes (pH 7.4) containing 0.15 M NaCl. The immobilization level was approximately 9000 RU. A new surface was prepared for every Biacore assay.

*Biacore Assays − General Conditions.* All the assays were run at room temperature in 0.01 M Hepes (pH 7.4) containing 0.15 M NaCl and 0.002 M $MgCl_2$ and consisted of 20 $\mu$g/mL dAK injection, followed by the injection of the reactants over the anti-His antibody surface. The enzyme, diluted in the running buffer, was captured at a flow rate 10 $\mu$L/min by means of the His-tag on one spot of the flow cell and the anti-His antibody on the second spot was used as an immobilized reference (in Biacore S51). In the experiments devised to obtain information about the composition of the reaction mixture (in Biacore 3000), the enzyme was captured on one flow cell, as described above, and the assays were conducted without using the reference surface. The reactants, dissolved in the running buffer, were injected at flow rate 30 $\mu$L/min. The capture of the enzyme on the covalently immobilized antibody resulted in the response increase with about 1800 RU. The antibody surface was regenerated after every cycle with 0.01 M glycine-HCl (pH 1.5).

## RESULTS

*Burst Kinetics.* To examine whether the dAK-catalyzed phosphorylation mechanism follows the biphasic kinetic scheme, a pre-steady-state kinetic analysis of the dGuo phosphorylation was performed under conditions in which the substrate was in slight molar excess over the enzyme. dGuo was selected because of its lowest $k_{cat}$ value (*3*).

Figure 1 shows the biphasic kinetics of the formation of dGMP during the course of the reaction. The observed burst rate and the observed steady-state rate are $1.3 \pm 0.5$ s$^{-1}$ and $0.09 \pm 0.07$ s$^{-1}$, respectively. Despite the high value of the standard errors caused by this rough-and-ready method of measurement, the biphasic character of the reaction is very clear.

*Analysis of the Reaction Mixture.* The analyte recovery feature of Biacore 3000 was used to elute the reaction mixture from the chip (Figure 2A). Two types of recovery experiments were performed: (i) a mixture of 1 mM ATP and 1 mM tritium-labeled dAdo was injected over dAK and the incubation time was varied from 10 to 600 s in nine consecutive experimental cycles; (ii) the incubation time was kept constant at 1 min and a concentration series of tritium-labeled dAdo (2−1000 $\mu$M) was injected over the enzyme in the presence of 1 mM ATP. The eluted material was collected in the tubes containing 1 M HCl to stop the reaction, then neutralized with 2 M NaOH, and spotted onto the DE-81 filter paper. The filter paper was then dried, washed, eluted, and counted, as described in Materials and Methods.

The results show (i) the time-dependent product formation on the sensor chip (Figure 2B), and (ii) the high activity of the immobilized enzyme, manifested by the $K'_m$ of dAdo estimated to 15 $\mu$M (Figure 2C).

*Product Binding Studies.* The binding of 2′-deoxyadenosine 5′-monophospate (dAMP) and adenosine 5′-diphosphate (ADP) to dAK was studied by injecting a series of product concentrations ranging from 35 to 600 $\mu$M over dAK. The injection of dAMP gave a set of curves showing a slow, but very stable, binding of this product to dAK (Figure 3). The association and dissociation rate constants for this interaction were estimated by fitting the binding curves to a bimolecular binding model with a mass transport term (*17*). The values

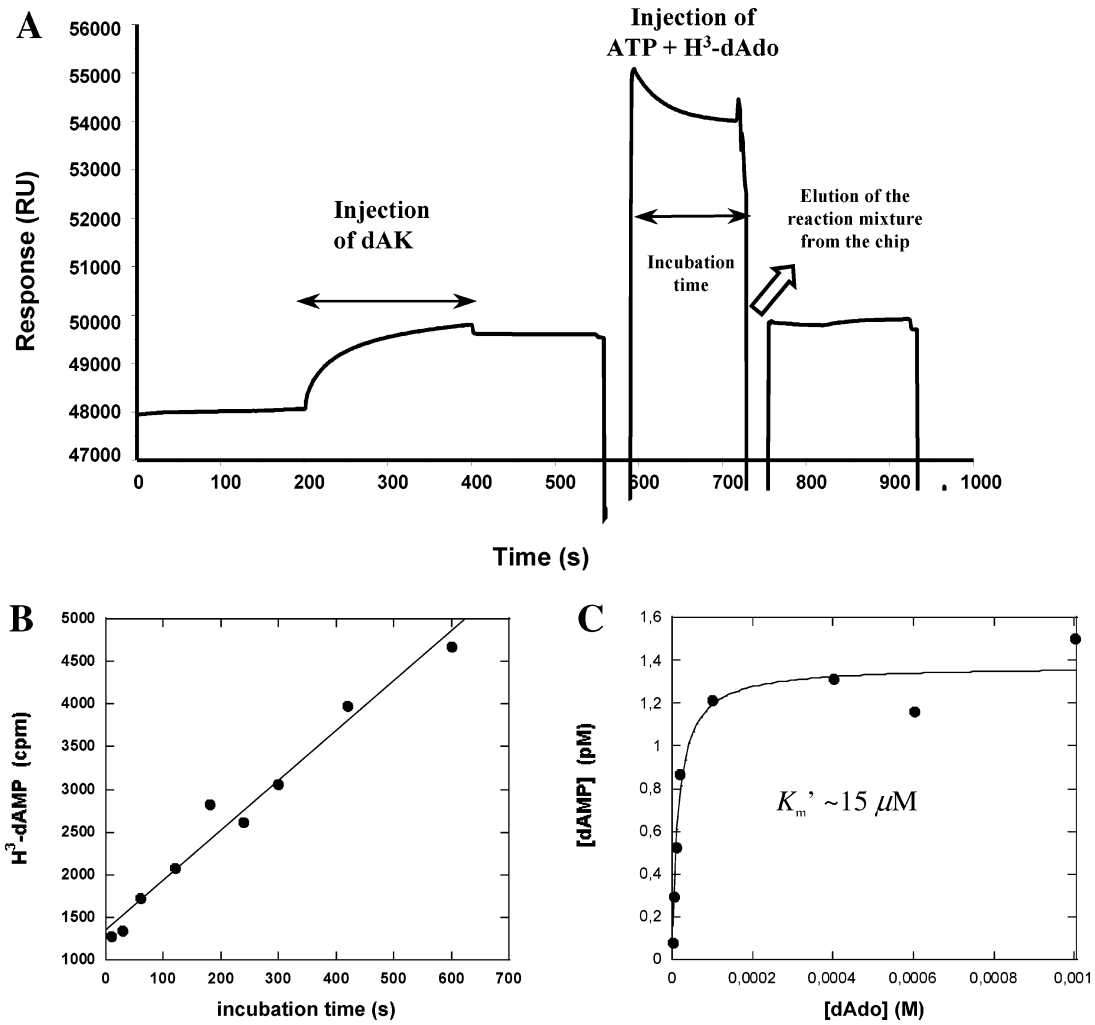


FIGURE 2: Showing that an enzymatic reaction occurs on the sensor surface. (A) A real-time monitoring of events on the sensor chip in Biacore 3000: the injections of dAK and of 1 mM ATP together with tritium-labeled dAdo are shown. The presence of the product in the eluted samples was examined using the DE-81 filter paper technique. (B) A linear dependence of product formation against time, when a mixture of ATP and 1 mM $H^3$-dAdo was incubated during an increasing period of time. (C) $K'_m$ for dAdo was estimated to 15 $\mu$M, when a concentration series of $H^3$-dAdo (2−1000 $\mu$M) was incubated 1 min with ATP and the amount of dAMP formed was determined.

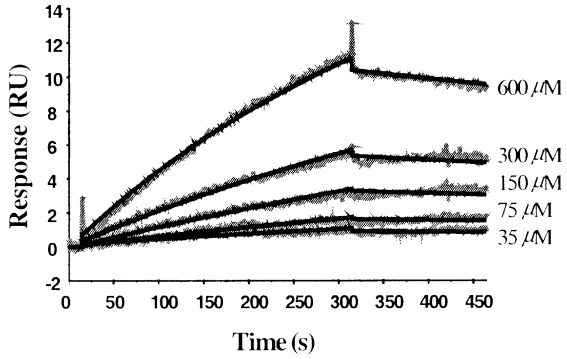


FIGURE 3: The binding curves representing the interaction of dAMP (concentration series 35−600 $\mu$M) with immobilized dAK. The data are fitted globally to a 1:1 interaction model with a mass transport term, yielding association and dissociation rate constants of (3.25 $\pm$ 0.01) $\times$ $10^{-1}$ $M^{-1}$ $s^{-1}$ and (5.43 $\pm$ 0.21) $\times$ $10^{-4}$ $s^{-1}$, respectively.

obtained were (3.25 $\pm$ 0.01) $\times$ $10^{-1}$ $M^{-1}$ $s^{-1}$ and (5.43 $\pm$ 0.21) $\times$ $10^{-4}$ $s^{-1}$, for the association and the dissociation rate constants, respectively, yielding the dissociation equilibrium constant of 1.67 mM (Figure 3). The injection of ADP over the dAK surface showed no binding.

*Determination of Michaelis−Menten Constants.* The $K'_m$ values for ribonucleoside triphosphates: ATP, CTP, TTP, and UTP with concentrations ranging from 5 to 2000 $\mu$M were determined in the presence of 1 mM 2′-deoxyadenosine (dAdo) in running buffer. Similarly, the $K'_m$ values for deoxyribonucleosides: dAdo, dGuo, and dCyd, with concentrations ranging from 2 to 1500 $\mu$M, were determined in the presence of 1 mM ATP or CTP in running buffer. The injection of the substrate pair of dAK over the enzyme resulted in the increased SPR responses. The sets of curves (sensorgrams), corresponding to the concentration series of the substrate, were prepared for evaluation by subtracting the reference surface and the running buffer signals. The sensorgrams were aligned at the point approximately 1−2 s after the substrate injection (Figure 4). The linear slopes of the initial linear portions of the curves were measured and plotted against the concentration of the substrates. The $K'_m$ values were determined by fitting the plots to the Michaelis−Menten equation (eq 5), using a nonlinear least-squares analysis (Figure 4).

The $K'_m$ values obtained are in good agreement with those obtained previously (*3*), as shown in Table 1. The use of

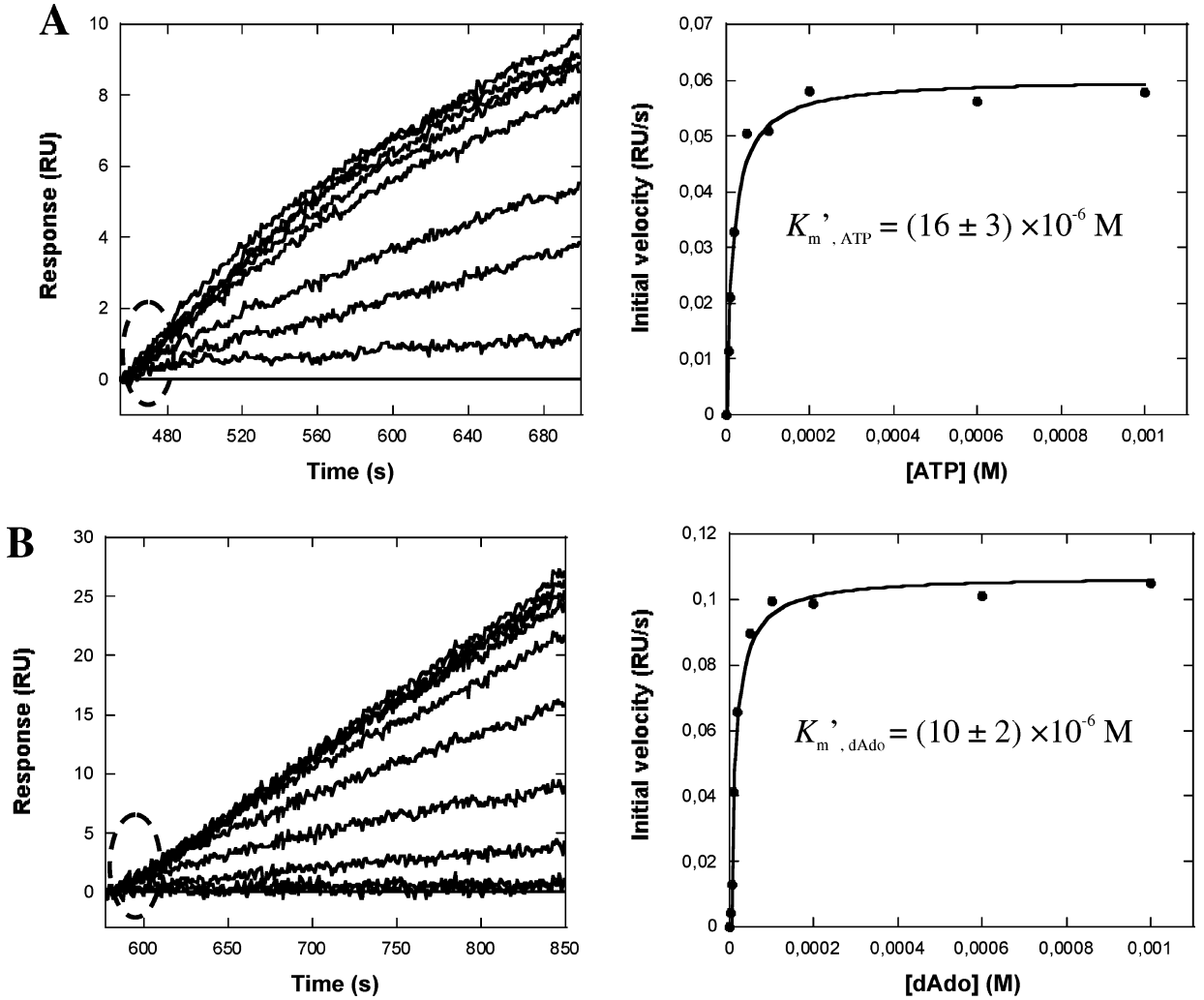


FIGURE 4: Determination of the $K'_m$ values − examples. A concentration series of (A) ATP (5−1000 $\mu$M) or (B) dAdo (2−1000 $\mu$M) were injected in the presence of excess of dAdo and ATP, respectively, over the dAK surface. The sets of curves, corresponding to the concentration series, were prepared for the evaluation by subtracting the reference surface and the running buffer signals. Initial slopes, marked with dotted ovals, were plotted against the substrate concentrations, and the plots were fitted to the Henry−Michaelis−Menten equation (eq 5). The fitted parameter, $K'_m$, is reported ± the standard errors.

CTP as an alternative phosphate group donor to ATP has only a moderate effect on the $K'_m$ values of deoxyribonucleosides (Table 1).

*Bi-Substrate Kinetic Analysis.* Bi-substrate initial rate patterns were analyzed to distinguish between a sequential and ping-pong mechanism (*7*, *9*). The analysis was performed for dAdo concentrations ranging from 5 to 1000 $\mu$M at four fixed nonsaturated ATP concentrations: 5, 20, 50, and 100 $\mu$M. The curves were prepared for evaluation as above. The initial binding velocities were obtained as the linear slopes of the initial linear portions of the curves and plotted against dAdo concentrations in a double-reciprocal format. The plot was fitted to the linear equation by a least squares linear regression analysis. The slopes and intercepts of the linear fits were re-plotted against the reciprocals of the ATP concentrations.

The double-reciprocal plot shows an intersecting pattern that is characteristic of the Bi Bi sequential mechanism (Figure 5A), in which both substrates have to bind to the enzyme before catalysis can occur (*7*−*11*). The lines intersect to the left of the vertical axis, approximately on the horizontal axis, indicating that the dissociation equilibrium constant and the Michaelis−Menten constant of the enzyme−dAdo complex, $K_{i,ATP}$ and $K'_{m,ATP}$, are of the same order of magnitude (*7*−*11*). The $K_{i,ATP}$ and $K'_{m,ATP}$ values, estimated from the crossing points with the horizontal axes of the re-plots (*7*−*11*), are ∼24 and ∼22 $\mu$M, respectively (Figure 5B).

*Product Inhibition Studies.* To decide whether the kinetic mechanism is Bi Bi ordered or Bi Bi random sequential (*7*−*11*), a product inhibition study was performed at the saturated level of the fixed substrate to ensure the best measurable initial slopes. Continuous delivery of this substrate to the sensor surface sustained truly saturated conditions. One concentration series, containing the varied substrate only, was included into each inhibition assay for comparison. Product inhibition studies with dAdo as varied substrate (concentrations ranged from 5 to 1300 $\mu$M), were performed at three concentrations, 30, 60, and 120 $\mu$M, of ADP and with 1 mM ATP in running buffer. The sensorgrams obtained were prepared for evaluation, and the initial velocities were measured, plotted against the dAdo concentrations in the reciprocal format, and fitted to the linear equation as above.

The double reciprocal initial binding rate pattern shows parallel lines with intercepts inversely proportional to the inhibitor concentrations (Figure 6A). According to the proposal offered in Theoretical Background, the pattern

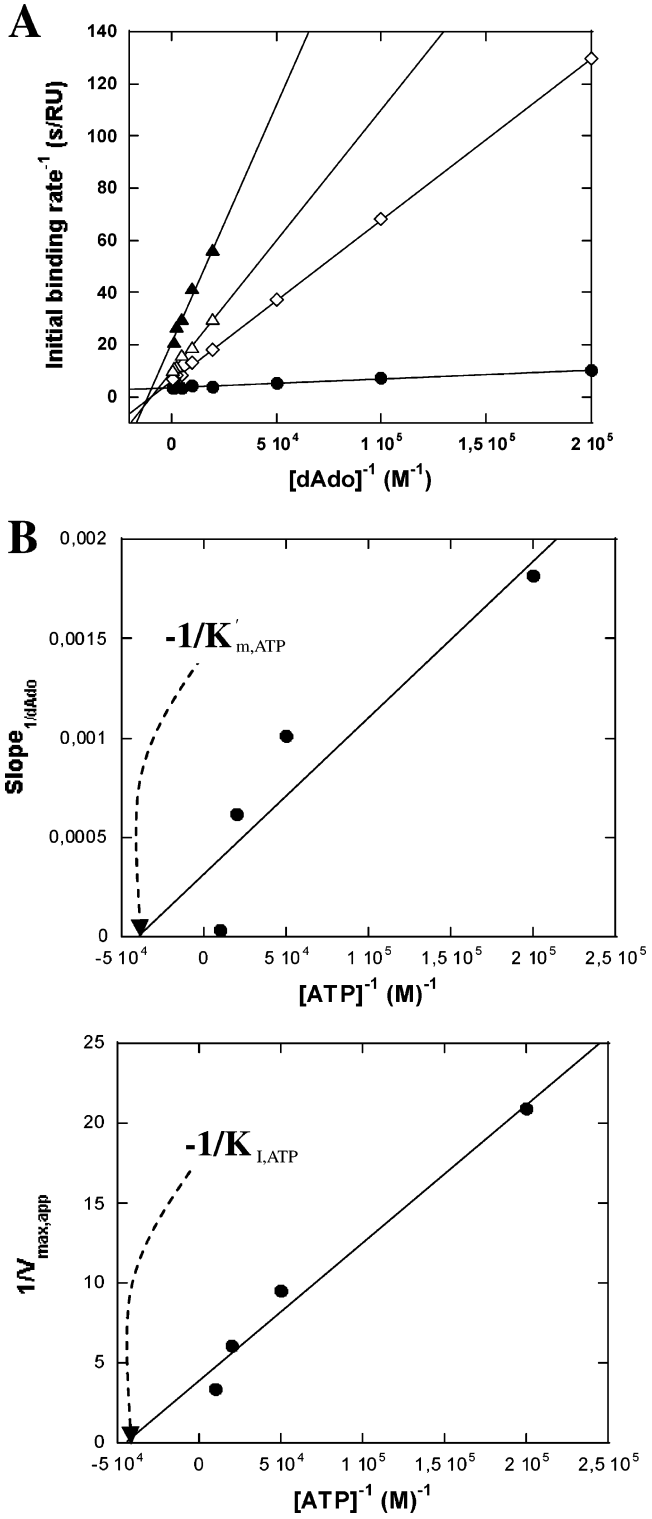


FIGURE 5: Determination of initial rate pattern. (A) Double reciprocal presentation of initial binding velocities when dAdo concentration series (5−1000 $\mu$M) were injected at four fixed ATP concentrations: ▲, 5 $\mu$M ATP, Δ, 20 $\mu$M ATP, ◇, 50 $\mu$M ATP, ●, 100 $\mu$M ATP. (B) Slope$_{1/dAdo}$ and $1/V_{max,app}$ re-plots against inverse ATP concentrations. The intercepts on $[ATP]^{-1}$ − axes give $K_{I,ATP} = 24$ $\mu$M and $K'_{m,ATP} = 22$ $\mu$M.

obtained indicates a noncompetitive inhibition mechanism. The dissociation equilibrium constant of the enzyme−ADP complex, estimated from the intercepts of the plot using eq 13, is about 200 $\mu$M.

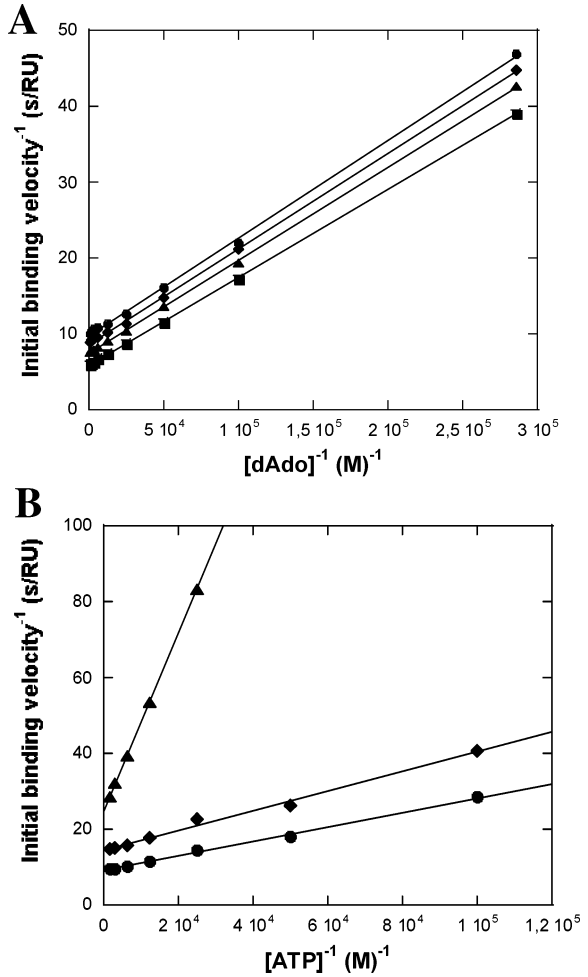


FIGURE 6: Determination of inhibitions patterns. Initial binding rates were plotted against the concentration of varied substrate in the reciprocal format and fitted to a linear equation. (A) ADP inhibition versus dAdo in the excess of ATP. dAdo concentration series (5−1300 $\mu$M) were injected in the absence of ADP and in the presence of several ADP concentrations: ●, no ADP added, ◆, 30 $\mu$M ADP, ▲, 60 $\mu$M ADP, ■, 120 $\mu$M ADP. The parallel lines indicate a noncompetitive inhibition mechanism (eq 13) with the affinity of the enzyme−ADP complex of ∼200 $\mu$M. (B) ADP inhibition versus ATP in the excess of dAdo. ATP concentration series (5−700 $\mu$M) were injected in the excess of dAdo, in the absence and in the presence of ADP: ●, no ADP added, ◆, 30 $\mu$M ADP, ▲, 60 $\mu$M ADP. The lines with varying slopes and intercepts suggest the uncompetitive inhibition mechanism (eq 17), in which the inhibitor binds directly to the enzyme−substrate complex with the affinity constant of ∼110 $\mu$M.

When 120 $\mu$M dAMP was used as the product-inhibitor under the conditions described above, the product binding pattern did not change, thus suggesting that this product does not act as an inhibitor versus dAdo.

Product inhibition studies with ATP as varied substrate were performed as above but in the presence of two concentrations, 30 and 60 $\mu$M of ADP or 60 and 120 $\mu$M of dAMP, with ATP concentrations ranging from 5 to 700 $\mu$M and with 1 mM dAdo in running buffer. The binding curves obtained were evaluated as above.

Both products affect the binding of ATP to the enzyme, yet in different ways. The double reciprocal pattern, obtained from the binding curves with ADP as the product-inhibitor, shows the lines with varying slopes and intercepts (Figure 6B), thus indicating the existence of the uncompetitive

inhibition in which the inhibitor binds to the enzyme simultaneously with the substrate (see Theoretical Background). The dissociation equilibrium constant of the (dAK−ATP)−ADP complex is approximately 110 $\mu$M, irrespective of whether it is calculated from the slopes or from the intercepts of the double reciprocal pattern using eq 17.

When dAMP is used as the product-inhibitor, the initial rate of product formation increases only very slightly at the lowest ATP concentration, and the use of 60 or 120 $\mu$M dAMP makes no appreciable difference on the curves (data not shown). Although such a behavior may indicate a competitive inhibition for the case when $K_I \gg K'_m$, it provides no conclusive evidence for this type of inhibition. Nevertheless, the $K_{I,dAMP}$ and $K'_{m,ATP}$ values, determined in this work from the separate experiments (Figures 3 and 4A), are 1.67 mM and 16 $\mu$M, respectively (i.e., $K_I \gg K'_m$ ). This indicates that the competitive inhibition actually takes place in this case.

## DISCUSSION

dAK belongs to the deoxycytidine kinase/deoxyguanosine kinase (dCK/dGK) enzyme family with broad substrate specificity regarding both phosphate acceptors and donors (*1*, *2*). The core structure of the dCK/dGK enzyme family consists of a phosphate-binding loop, a lid structure that is involved in phosphate transfer, and a substrate-binding pocket (*18*). In the literature, controversial kinetic mechanisms have been proposed for human dCK. An ordered sequential pathway, with ATP being the first substrate to bind and dCMP the last product to dissociate, was determined for dCK purified from leukemic T-lymphoblasts (*19*). A rapid equilibrium random Bi Bi mechanism with a possible formation of dead-end complex of the enzyme with ATP as phosphate donor (*20*) and a mechanism with sequential binding of the substrates and random release of the products with UTP as the phosphate donor (*21*), were proposed for dCK prepared from MOLT-4 T-lymphoblasts. For the dGK enzymes, a rapid-equilibrium random Bi Bi kinetic mechanism, which may include the formation of a dead-end complex, was proposed for the bovine liver mitochondrial dGK (*22*), whereas an ordered Bi Bi reaction mechanism, with UTP as the leading substrate and UDP as the last product to leave, was proposed for the *Bacillus subtilis* dGK (*23*).

In this paper, we investigate the kinetic mechanism of dAK using the fast, convenient, and label-free Biacore assays, which combine the initial rate studies with product binding experiments. First, we establish that the catalytic reaction in fact occurs on the sensor surface and that the activity of the immobilized enzyme is close to that of the enzyme in solution (Figure 2). Second, we demonstrate that the dissociation of deoxyribonucleoside monophosphate is the rate-limiting step of the reaction (Figures 1 and 3). These experiments show that our method for studying the enzymatic activity of dAK on the sensor surface must be considered highly reliable.

The conclusion to be drawn from the analysis of the bisubstrate initial rate pattern is that the mechanism is of the Bi Bi sequential type (Figure 5). The product inhibition study, performed to establish the nature of this mechanism, suggests that, at the saturating level of the fixed substrate, ADP is the noncompetitive inhibitor of dAdo (Figure 6A) and the uncompetitive inhibitor of ATP (Figure 6B), whereas dAMP

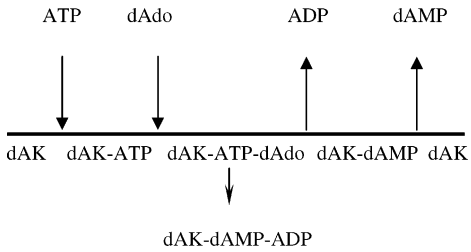


FIGURE 7: Proposed kinetic mechanism of deoxyadenosine kinase (dAK).

is not an inhibitor of dAdo. Despite not being explicitly informative of how dAMP acts as an inhibitor versus ATP, the inhibition pattern described is distinctive of Bi Bi sequential ordered mechanism. In this kinetic mechanism, ATP binds first, followed by dAdo and a subsequent transfer of the phosphate group, and an ordered release of products with ADP dissociating before dAMP (Figure 7). The product binding study that shows the binding of dAMP, but not of ADP, to the free enzyme, strongly supports this conclusion.

According to the mechanism proposed, substrate ATP and product dAMP can only bind to the free enzyme and, consequently, the binding of one of them prevents the other from binding to dAK. When dAMP was used as product inhibitor with dAdo as varied substrate, no inhibition could be observed, because the inhibitor was completely competed out by the saturated amount of ATP being the fixed substrate. All the available dAK was incorporated into the complex with ATP, which precluded the binding of dAMP. This product inhibition experiment also indicates that dAMP is a competitive inhibitor of ATP.

Our results suggest that ATP binds to the enzyme first and, in the course of the dAK−ATP complex formation, the enzyme undergoes a conformational change to an open state, thereby facilitating the binding of dAdo. In the process, the ADP binding site can emerge, which in turn can lead to the formation of the dAK−ATP−ADP complex. Consequently, although ADP normally binds to the dAK−dAMP complex, it can even bind to the dAK−ATP complex, in both cases acting as an uncompetitive inhibitor of ATP. When both ATP and dAdo are bound, the enzyme assumes the form of a closed state and the phosphate transfer occurs. Once the products are formed, the enzyme conformation changes to another open state and ADP leaves the enzyme before dAMP, thus completing a reaction cycle. The noncompetitive inhibition, observed when ADP was used as an inhibitor versus dAdo, is consistent with the dAdo and ADP binding to dAK−ATP and dAK−dAMP complexes, respectively.

The reaction mechanism, described above, appears to involve dynamic conformational changes. A detailed understanding of this mechanism may help to design specific inhibitors of dAK that could either interfere with the binding of substrates or bind to the enzyme−substrate/product intermediate thus blocking the reaction. The 3-D structure determination of dAK, which is in progress, can give further insights into the relationship between the enzyme structure and its mechanism of action.

## ACKNOWLEDGMENT

We want to express our gratitude to Francis Markey, Biacore AB, for critically reading the manuscript and providing us with numerous valuable comments. We would

also like to thank Prof. Ingemar Björk for stimulating discussions on the subject. In the course of our investigations, we have greatly profited from the EMBO Practical Course on Transient Kinetics Applied to Biological Macromolecules, Canterbury, U.K., 2000.

## REFERENCES

1. Arner, E. S. J., and Eriksson, S. (1995) Mammalian deoxyribonucleoside kinases, *Pharm. Ther. 67*, 155−186.
2. Eriksson, S., and Wang, L. (2002) The role of the cellular deoxynucleoside analogs used in chemotherapy, in *Recent Advances in Nucleosides: Chemistry and Chemotherapy* (Chu, C. K., Ed.) Elsevier, Amsterdam, 455−475.
3. Wang, L., Westberg, J., Bölske, G., and Eriksson, S. (2001) Novel deoxynucleoside-phosphorylation enzymes in mycoplasma: evidence for efficient utilization of deoxynucleosides, *Mol. Microbiol. 42*, 1065−1073.
4. Jonsson, U., Fägerstam, L., Ivarsson, B., Johnsson, B., Karlsson, R., Lundh, K., Löfas, S., Persson, B., Roos, H., Rönnberg, I., et al. (1991) Real-time biospecific interaction analysis using surface plasmon resonance and a sensor chip technology, *Biotechniques 11*, 620−627.
5. Karlsson, R., Michaelsson A., and Matsson, L. (1991) Kinetic analysis of monoclonal antibody−antigen interactions with a new biosensor based analytical system, *J. Immunol. Methods 145*, 229−240.
6. Stenberg, E., Persson, B., Roos, H., and Urbaniczky, C. (1991) Quantitative determination of surface concentration of protein with surface plasmon resonance using radiolabeled proteins, *J. Colloid Interface Sci. 143*, 513−526.
7. Segel, I. H. *Enzyme Kinetics*: *Behavior and Analysis of Rapid Equilibrium and Steady-State Enzyme Systems*, Wiley Classics Library Edition, Wiley, New York, 1993.
8. Cleland, W. W. *Steady-State Kinetics*, in (Boyer, P. D., Ed.) *The Enzymes*, Vol. 2., 3rd ed., pp 1−65, Academic Press, New York.
9. Cleland W. W. (1977) Determining the chemical mechanism of enzyme-catalyzed reactions by kinetic studies, *Adv. Enzymol. 45*, 273−387.
10. Cleland, W. W. (1986) Enzyme kinetics as a tool for determination of enzyme mechanisms, *Techn. Chem. 6*, 791−870.
11. Fromm, H. J. (1979) Summary of kinetics reaction mechanisms, *Methods Enzymol. 63*, 42−53.
12. Haldane, J. B. S. (1930) *Enzymes*, The MIT Press, Cambridge, MA.
13. Gutfreund H. (1998) *Kinetics for the Life Sciences*, Cambridge University Press, Cambridge, UK.
14. Glaser, R. W. (1993) Antigen−antibody binding and mass transport by convection and diffusion to a surface: A two-dimensional computer model of binding and dissociation kinetics, *Anal. Biochem. 213*, 152−161.
15. Karlsson, R. (1994) Real-time competitive kinetic analysis of interactions between low-molecular-weight ligands in solution and surface-immobilized receptors, *Anal. Biochem. 221*, 142−151.
16. *Biacore Sensor Surface Handbook*, version AA, BR-1005-71, Biacore, Uppsala, Sweden, 2003.
17. Karlsson R. (1999) Affinity analysis of non-steady-state data obtained under mass transport limited conditions using BIAcore technology, *J. Mol. Recognit. 12*, 285−292.
18. Eriksson, S., Munch-Petersen, B., Johansson, K., and Eklund, H. (2002) Structure and function of cellular deoxynucleoside kinases, *Cell. Mol. Life Sci. 59*, 1327−1346.
19. Kim, M.-Y., and Ives, D. H. (1989) Human deoxycytidine kinase: kinetic mechanism and end product regulation, *Biochemistry 28*, 9043−9047.
20. Datta, N. S., Shewach, D. S., Mitchell, B. S., and Fox, I. H. (1989) Kinetic properties and inhibition of human T lymphoblast deoxycytidine kinase, *J. Biol. Chem. 264*, 9359−9364.
21. Hughes, T., Hahn, T., Reynolds, K., and Shewach, D. (1997) Kinetic analysis of human deoxycytidine kinase with the true phosphate donor uridine triphosphate, *Biochemistry 36*, 7540−7547.
22. Park, I., and Ives, D. H. (1995) Kinetic mechanism and end-product regulation of deoxyguanosine kinase from beef liver mitochondria, *J. Biol. Chem. 117*, 1058−1061.
23. Andersen, R., and Neuhard, J. (2001) Deoxynucleoside kinases encoded by the yaaG and yaaF genes of *Bacillus subtilis*. Substrate specificity and kinetic analysis of deoxyguanosine kinase with UTP as the preferred phosphate donor, *J. Biol. Chem. 276*, 5518−5524.

BI0515523